Quantum transport in a one-dimensional quasicrystal with mobility edges

Yan Xing,[1] Lu Qi,[1] Xuedong Zhao,[1] Zhe Lü,[1,*] Shutian Liu,[1] Shou Zhang,[2,†] and Hong-Fu Wang [2,‡]

[1]*School of Physics, Harbin Institute of Technology, Harbin, Heilongjiang 150001, China*
[2]*Department of Physics, College of Science, Yanbian University, Yanji, Jilin 133002, China*

Quantum transport in a one-dimensional (1D) quasiperiodic lattice with mobility edges is explored. We first investigate the adiabatic pumping between left and right edge modes by resorting to two edge-bulk-edge channels and demonstrate that the success or failure of the adiabatic pumping depends on whether the corresponding bulk subchannel undergoes a localization-delocalization transition. Compared with the paradigmatic Aubry-André model, the introduction of mobility edges triggers an opposite outcome for successful pumping in the two channels, showing a discrepancy of the critical condition, and facilitates the robustness of the adiabatic pumping against quasidisorder. We also consider the transfer between excitations at both boundaries of the lattice, and an anomalous phenomenon characterized by the enhanced quasidisorder contributing to the excitation transfer is found. Furthermore, there exists a parametric regime where a nonreciprocal effect emerges in the presence of mobility edges, which leads to a unidirectional transport for the excitation transfer and enables potential applications in the engineering of quantum diodes.

I. INTRODUCTION

Anderson localization [1–3], a fundamental and ubiquitous phenomenon in nature, describes the absence of electron diffusion and the nonergodicity of electronic Bloch waves aroused by disorder, which originates from destructive quantum interference and uncovers the underlying mechanism behind metal-insulator transitions [4,5]. According to the scaling theory of localization [6], while arbitrarily small random (uncorrelated) disorder in both one and two dimensions produces spatially exponential localization for all single-particle states, a localization-delocalization transition exists in higher dimensions, and an energy-dependent mobility edge distinguishing the localized regime from the delocalized regime appears at the phase boundary. However, this picture is altered dramatically in quasicrystals [7–10] when the random disorder is replaced with a quasiperiodic potential. One of the most celebrated examples is characterized by the one-dimensional (1D) Aubry-André (AA) model [11–13], which displays such an energy-independent critical behavior at a self-dual point. Moreover, rapid developments and remarkable advances in the manipulation of ultracold atoms loaded into incommensurate bichromatic optical lattices have led to a powerful tool to experimentally realize the AA model [4,14–17]. Interestingly, by incorporating longer-range hopping [18–24] or appropriately designing on-site modulation [25–27], some modified AA models can also sustain energy-dependent mobility edges. Recently, experimental observations of mobility edges were also reported in ultracold-atom systems [28–30].

On the other hand, quasicrystals exhibit a topologically nontrivial phase [31–33] that is attributed to higher-dimensional systems [34]; for instance, the 1D AA model under an open boundary geometry supports gapless end modes spanning the bulk gaps, which are equivalent to the edge modes in the two-dimensional quantum Hall effect [35]. With the concept of topological protection in mind, these modes localized on the open boundary are immune to local perturbations and disorder, such as thermal fluctuations and defects, making them a promising candidate for exploiting noise-resistant quantum information processing [36,37] and fault-tolerant quantum computation [38,39]. More importantly, from a dynamical point of view, perhaps Thouless pumping [40–44], the quantization of the excitation transport, which occurs if the parameters of the system are adiabatically tuned in a cyclic manner, is the most visual reflection of the nontrivial topology of the system since the generated quantized excitation transport per cycle is in response to the topological invariants of the system. Furthermore, the topological pumping of boundary modes [34,45–51] can be another significant domain and has attracted intensive attention. It also depends on an adiabatic adjustment of the parameters of the system and dedicates excitation transport across the bulk, which opens up avenues for robust quantum state transfer [52–65], resilient quantum gate preparation [66], etc.

Although the investigation of these basic principles and essential properties has led to substantial progress in their respective realms, the interplay among them still remains less explored. For example, the effect of Anderson localization and mobility edges on the adiabatic pumping between boundary modes is still not explicitly understood and has not been clarified, and the way mobility edges further affect the excitation transport has not been clearly demonstrated yet; quasicrystals provide an ideal platform to address these problems.

Motivated by the confusion, in this work, we explore quantum transport in a 1D quasiperiodic lattice with mobility edges. First, the adiabatic pumping between left and right

*lvzhe@hit.edu.cn
†szhang@ybu.edu.cn
‡hfwang@ybu.edu.cn

032443-1

edge modes is investigated by resorting to two edge-bulk-edge channels, which is always feasible before Anderson localization of the corresponding bulk subchannel occurs, and the relevant cause for the failure of the adiabatic pumping in the localized regime is analyzed and discussed in detail. Compared with the AA model in which successful pumping in both channels can be achieved until the system undergoes a localization-delocalization transition, the opposite outcome for successful pumping in the two channels is realized after mobility edges are introduced: while one channel can survive only under a reduced critical condition, the other can persist beyond the constraint of the AA model, which, in a sense, indicates the presence of mobility edges facilitates the robustness of the adiabatic pumping against quasidisorder. Depending on the pumping process, the transfer between excitations at both boundaries of the lattice is also considered and is found to be anomalous in the delocalized regime, showing the enhanced quasidisorder raises the fidelity of the excitation transfer. Moreover, there exists a parametric regime where nonreciprocal transport manifested by the unidirectional excitation transfer is captured, which is induced by the mobility edges and cannot emerge in the AA model.

The remainder of this paper is organized as follows. In Sec. II, we introduce the model and present the existence of mobility edges for a sample system. In Sec. III, for both the delocalized and localized regimes, the adiabatic pumping between the left and right edge modes in the AA model is first explored by resorting to two edge-bulk-edge channels, where we analyze in detail and discuss what determines the success or failure of the adiabatic pumping in terms of the energy spectrum of the system. Subsequently, the adiabatic pumping in the sample system is shown, and the effect of the mobility edges on the adiabatic pumping in each channel is expounded. We also quantify the pumping outcome based on the fidelity. In Sec. IV, from the perspective of the application of the adiabatic pumping, we consider the transfer between excitations at both boundaries of the lattice, where some novel transport phenomena are found. A conclusion is given in Sec. V.

II. MODEL AND MOBILITY EDGES

We consider a 1D shallow bichromatic optical lattice where the ratio between the periods of the primary and secondary cosine potentials is incommensurate, so that the non-nearest-neighbor tight-binding framework is released, and a lattice model subject to short-range hopping can be attained [18–20]. Specifically, we focus on a lattice model characterized by exponentially decaying hopping, and the Hamiltonian of the system reads

$$H = \sum_{m \neq l} t e^{-u|m-l|} (a_m^\dagger a_l + a_l^\dagger a_m) + \sum_m w_m a_m^\dagger a_m, \quad (1)$$

where $a_m^\dagger$ (a_m) denotes the creation (annihilation) operator of a particle on site m. The exponentially decaying hopping is described by hopping amplitude t and decay coefficient $u > 0$. The on-site potential takes the quasiperiodic cosine modulation $w_m = V \cos(2\pi \zeta m + \varphi)$, with parameters $V > 0$, $\zeta^{-1} = (\sqrt{5} + 1)/2$, and $\varphi \in [0, 2\pi]$ being the modulation strength,
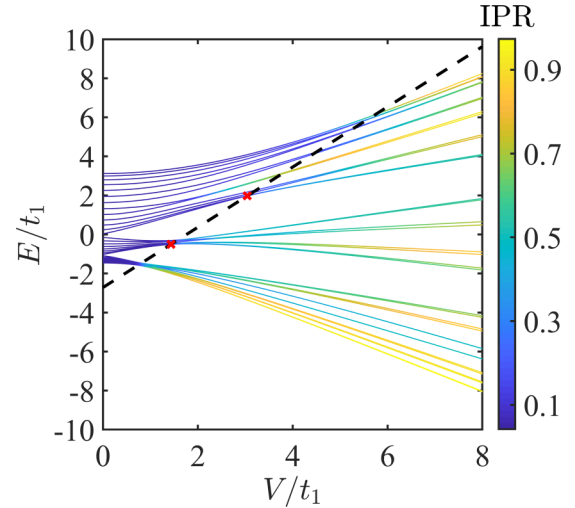

FIG. 1. Energy spectrum of a sample system with $u = 1$ versus modulation strength V for $\varphi = 0.99\pi$. The black dashed line delineates the analytical result of the mobility edge, which is validated according to the IPR of each eigenmode, as indicated by the color bar. The two red crosses mark the threshold V_c for the bulk subchannels of channels A and B.

period, and phase, respectively. The lattice model is just a simple short-range hopping counterpart of the AA model, and if there is only the hopping term $t_1 = t e^{-u}$, which is referred to as the energy unit throughout the paper, the lattice model will be reduced to the AA model. However, compared with the AA model, which undergoes a localization-delocalization transition determined by the self-dual condition $V_c = 2$, the lattice model satisfies a generalized self-dual symmetry and sustains energy-dependent mobility edges, which separate the localized regime from the delocalized regime at a critical energy E_c governed by $E_c = V_c \cosh(u) - t$ [19]. Figure 1 depicts the energy spectrum of a sample system versus V when $u = 1$, and the black dashed line delineates the analytical result of the mobility edge. The presence of the mobility edge is validated according to the inverse participation ratio (IPR) of each eigenmode, which is defined as

$$R_{IP} = \frac{\sum_{m=1}^N |\psi_m|^4}{\left(\sum_{m=1}^N |\psi_m|^2 \right)^2}, \quad (2)$$

where ψ_m stands for the probability amplitude of the corresponding eigenmode at the mth site and N is the total number of sites. One can readily confirm that $R_{IP} = 1$ for the most localized state and $R_{IP} = 1/N$ for the completely delocalized state. Visibly, the abrupt change in the IPR agrees well with the prediction of the mobility edge, which indicates that the localization-delocalization transition is indeed dictated by the mobility edge.

III. ROBUST ADIABATIC PUMPING FACILITATED BY MOBILITY EDGES

It is well known that the AA model supports topologically nontrivial edge modes that traverse the bulk gaps [34,35]. Under the open boundary condition (OBC), we present the energy spectrum of the AA model as a function of φ with
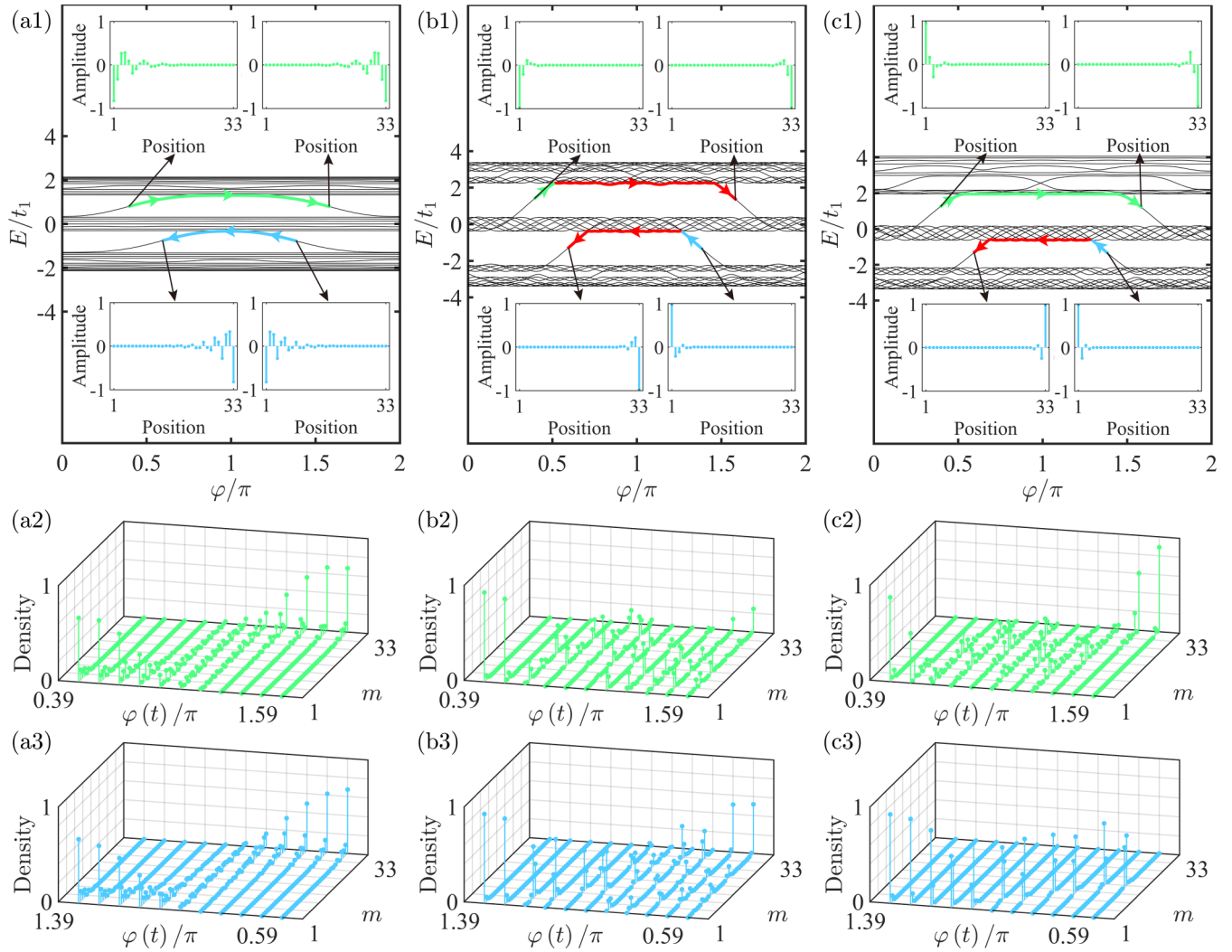
FIG. 2. Energy spectrum of the AA model with the number of sites $N = 33$ as a function of the modulation phase φ for (a1) $V = 1$ and (b1) $V = 3$. In (a1), the system is in the delocalized regime. The green (upper) and blue (lower) lines label channel A with $\varphi \in [0.39\pi, 1.59\pi]$ and channel B with $\varphi \in [0.59\pi, 1.39\pi]$ for an adiabatic pumping between the left and right edge modes, respectively. The arrows in each channel guide the corresponding pumping direction. In (b1), the system is in the localized regime. Both bulk and right edge subchannels break down in both channels, as indicated by the red (dark gray) line and arrow. (c1) Energy spectrum of the sample system as a function of the modulation phase φ. Other parameters are the same as in (b1). Channel A remains intact, but channel B collapses in this case. The insets in (a1)–(c1) display the initial left and goal right edge states used in the adiabatic evolution of each channel. The corresponding pumping process after resorting to (a2)–(c2) channel A and (a3)–(c3) channel B. Here, $\Omega = 10^{-5}$ in all the plots.

$V = 1$ in Fig. 2(a1). We can observe that there are two major gaps and gapless edge modes emerge within either gap. As displayed in the insets of Fig. 2(a1), the edge modes inside the upper (lower) gap are mainly concentrated on the left (right) boundary of the system if these modes cross from bottom to top, whereas the right (left) edge modes can be captured when the crossing direction is the opposite. Furthermore, these edge modes become extended gradually as they merge into the bulk sublevels on both sides. Clearly, these left and right edge modes inside the upper (lower) gap are bridged by a bulk sublevel, which is at the bottom of these upper (middle) sublevels.

Due to the existence of the gap between this bulk sublevel and its adjacent sublevel, the system in the delocalized regime admits an adiabatic pumping between the left and right edge

modes by engineering a relevant channel when φ is scanned sufficiently slowly. As an example, if we intend to pump a left edge mode to the right boundary of the lattice, there are two feasible channels to implement. As shown in Fig. 2(a1), one is labeled by the green (upper) line and called channel A, the other is labeled by the blue (lower) line and called channel B, and the arrows in each channel guide the corresponding pumping direction. We can divide either channel into three parts, namely, the left edge subchannel, bulk subchannel, and right edge subchannel. Because the region of the bulk subchannel for either channel becomes wider with the increase of V, in order to make the left and right edge subchannels always exist for each channel in the investigated range of V, for channel A (B), for example, φ is slowly swept from 0.39π (1.39π) to 1.59π (0.59π) with $\varphi(t) = 0.39\pi + \Omega t$

$[\varphi(t) = 1.39\pi - \Omega t]$, where t represents the evolution time and Ω is the ramping frequency dominating the evolution velocity; an adiabatic change in φ was experimentally realized in ultracold-atom systems [41,42]. We can obtain the pumping process by solving the Schrödinger equation numerically ($\hbar = 1$),

$$i\frac{d}{dt}|\Phi(t)\rangle = H(t)|\Phi(t)\rangle, \tag{3}$$

where $\Phi(t)$ is spanned by the basis $\{|m\rangle = a_m^\dagger |\mathbf{0}\rangle, 1 \leqslant m \leqslant N\}$, i.e., $\Phi(t) = \sum_{m=1}^{N} \phi_m(t)|m\rangle$, with $\phi_m(t)$ being the probability amplitude on the mth site at time t. The corresponding pumping processes after resorting to channels A and B are reported in Figs. 2(a2) and 2(a3), respectively. Obviously, for both channels, the whole pumping process undergoes three stages manifested by left-localized intensity → extended intensity → right-localized intensity, which means that the pumping entirely occupies each channel all the time and successively passes the three subchannels over the whole adiabatic evolution. Moreover, the left edge mode is pumped to the desired right edge mode successfully.

The Anderson localization occurs once $V > 2$ and all the bulk modes of the system become exponentially localized [12]. The energy spectrum of the AA model as a function of φ with $V = 3$ under the OBC is shown in Fig. 2(b1). Different from the energy spectrum in the delocalized regime, except for the two major gaps, the gap between each pair of sublevels in the localized regime is squeezed and becomes exponentially suppressed at multiple locations of φ, including the gap between each bulk subchannel and the adjacent sublevel, while the edge modes remain inside both major gaps and are unaffected, which, in a sense, reflects the sensitivity of a bulk mode without topological protection and the immunity of a topologically protected edge mode to quasidisorder. Moreover, the localization of these edge modes is enhanced, as displayed in the insets of Fig. 2(b1).

If the adiabatic pumping is executed again, we find that the pumping for both channels fails, as reported in Figs. 2(b2) and 2(b3). The underlying mechanism behind the failure of either pumping is attributed to the exponentially suppressed gap leading to the Landau-Zener tunneling between sublevels, and the tunneling probability depends on the size of the avoided crossing and on the evolution velocity. Concretely, the narrower the avoided crossing is or the faster the evolution velocity is, the larger the tunneling probability is. Therefore, the pumping completely enters into the bulk subchannel from the left edge subchannel. Subsequently, when the pumping first encounters the avoided crossing at an exponentially suppressed gap between the bulk subchannel and its adjacent sublevel, depending on the magnitude of both the avoided crossing at the exponentially suppressed gap and Ω, it could be subject to a partial or even whole tunneling from the bulk subchannel to its adjacent sublevel and further to the nonadiabatic excitation to the adjacent sublevel and thereby to the leak into the adjacent sublevel. The pumping will hence no longer occupy the bulk subchannel completely in later evolution. As evolution continues, whenever the pumping encounters the avoided crossing at an exponentially suppressed gap between sublevels, either a partial or whole Landau-Zener tunneling

between the two sublevels will occur. After undergoing a series of avoided crossings, there is a large possibility for the pumping to fail to return to the right edge subchannel perfectly, as labeled by the red (dark gray) line and arrow for each channel in Fig. 2(b1). Furthermore, an examination of these two pumping processes in Figs. 2(b2) and 2(b3) reveals the observation that the left-localized intensity transforms into several localized intensities at different sites of the lattice during evolution, which implies the occurrence of the Landau-Zener tunneling between sublevels and thus a simultaneous occupation of several exponentially localized bulk modes.

It can be seen from the above analysis and discussion that the bulk subchannel is fragile and breaks down in the localized regime, which is responsible for the failure of either pumping. Consequently, the adiabatic pumping between the left and right edge modes survives until the occurrence of the Anderson localization, or in other words, the adiabatic pumping is not robust against quasidisorder with disorder strength $V > 2$. In order to facilitate the robustness of the adiabatic pumping against quasidisorder, namely, achieving successful pumping under stronger quasidisorder, a crucial factor is to prevent the Landau-Zener tunneling from the bulk subchannel to its adjacent sublevel. Accordingly, a resolved gap between them should be guaranteed when $V > 2$, which requires raising the threshold V_c for their localization-delocalization transition such that they can still be in the delocalized regime after $V > 2$. On the other hand, with the introduction of the mobility edge, we can find in Fig. 1 that the thresholds of these upper (middle) sublevels are all greater (less) than 2. More importantly, the bulk subchannel of channel A (B) is at the bottom of these upper (middle) sublevels, whose V_c is approximately equal to 3.042 (1.434), as marked by the red cross. As a result, we will expect that successful pumping can always be achieved by resorting to channel A as long as $V < 3.042$, whereas the adiabatic pumping in channel B survives only before $V > 1.434$.

In Fig. 2(c1), we also plot the energy spectrum of the sample system as a function of φ with $V = 3$ under the OBC to verify the effect of the mobility edge on both bulk subchannels. We can observe that while the gaps within these middle sublevels all become exponentially suppressed and do not persist, the mobility edge maintains a resolved gap between every two upper sublevels, which demonstrates that the Anderson localization for these middle sublevels has already occurred but these upper sublevels have not undergone the localization-delocalization transition yet and are still in the delocalized regime. As a consequence, the bulk subchannel of channel A (B) remains intact (breaks down). Additionally, the corresponding pumping processes after resorting to channels A and B are reported in Figs. 2(c2) and 2(c3), respectively. As expected, the adiabatic pumping in channel B fails; nevertheless, the left edge mode is successfully pumped to the desired right edge mode by resorting to channel A, and successful pumping is indeed achieved when $V > 2$, which contrasts sharply with the case of the AA model with the same V shown in Fig. 2(b2).

For the purpose of elucidating the effect of the mobility edge on the adiabatic pumping more clearly, we introduce fidelity to quantitatively characterize the pumping outcome,
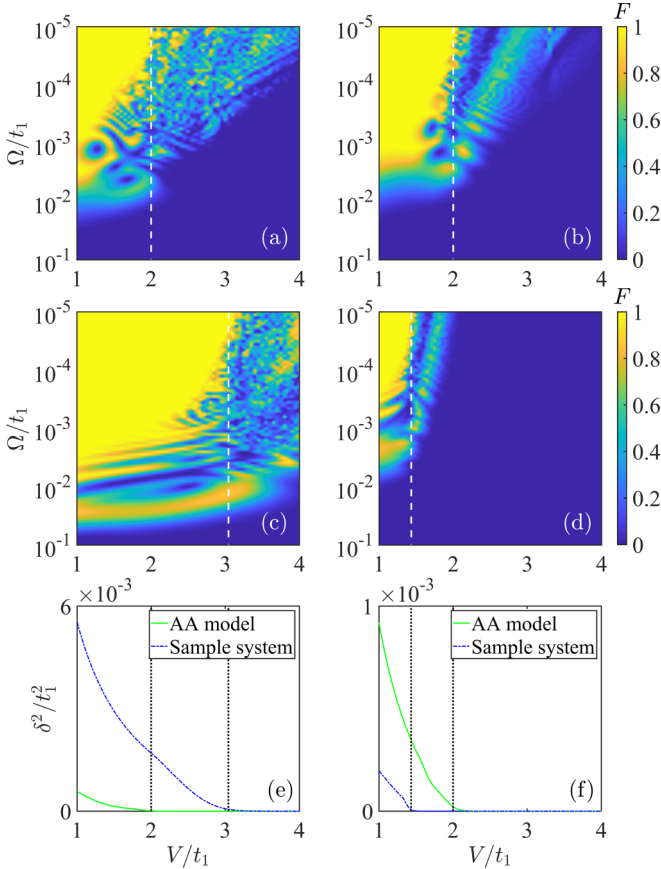
FIG. 3. Fidelity F of the adiabatic pumping between left and right edge modes versus modulation strength V and ramping frequency Ω via (a) channel A in the AA model, (b) channel B in the AA model, (c) channel A in the sample system, and (d) channel B in the sample system. The square of the minimum gap δ between the corresponding bulk subchannel and its adjacent sublevel as a function of modulation strength V for (e) channel A and (f) channel B of the AA model and sample system. The white dashed or black dotted lines in each plot delineate the threshold V_c of the corresponding bulk subchannel extracted from Fig. 1 or $V = 2$.

which can be evaluated as follows:

$$F = |\langle \Psi_g | \Psi_f \rangle|^2, \qquad (4)$$

where $|\Psi_f\rangle$ and $|\Psi_g\rangle$ are the normalized final state when the adiabatic evolution of an initial left edge state is finished and the normalized goal right edge state, respectively, and $0 \leqslant F \leqslant 1$. It is clear that $F \to 0$ indicates the failure of the pumping; on the contrary, the pumping is successful if $F \to 1$.

As a comparison, we first show the fidelities F of channels A and B versus V and Ω for the AA model in Figs. 3(a) and 3(b); the fidelities F of both channels versus V and Ω for the sample system are displayed in Figs. 3(c) and 3(d). Furthermore, for the AA model and sample system, Fig. 3(e) [Fig. 3(f)] exhibits the square of the minimum gap δ between the bulk subchannel of channel A (B) and its adjacent sublevel as a function of V. The white dashed or black dotted lines in each plot delineate V_c of the corresponding bulk subchannel extracted from Fig. 1 or $V = 2$. We can observe that for the AA model, if Ω is small enough (corresponding to a

sufficiently adiabatic pumping process), successful pumping in both channels can be achieved until the system undergoes the localization-delocalization transition, viz., when $V < 2$. For the sample system, by resorting to channel A, if $V < 3.042$, i.e., before the corresponding bulk subchannel suffers the Anderson localization, successful pumping always persists provided that the evolution velocity is sufficiently slow; however, despite the adiabatic pumping in channel B also surviving until the occurrence of the Anderson localization of the corresponding bulk subchannel, we can realize it only before $V > 1.434$. Moreover, as V increases, we find that the minimum Ω required for successful pumping dwindles, which is rooted in the decline of δ^2 such that a longer temporal evolution is necessary. In the localized regime, due to the almost vanishing δ^2, the pumping nearly fails without a very high fidelity no matter how small Ω becomes. In other words, the mobility edge plays a pivotal role in improving the fragility of the bulk subchannel of channel A and facilitates the robustness of the adiabatic pumping against quasidisorder.

Note that finite-time nonadiabatic excitations always exist during evolution; therefore, it is not possible to have perfect pumping $F = 1$. However, in the delocalized regime, all of the fidelities in the region of successful pumping are greater than 0.99, and we can thus ignore these very few nonadiabatic excitations.

It is worth mentioning that in the delocalized regime, as the size of the system increases, the gap between each bulk subchannel and its adjacent sublevel gradually shrinks but still persists, unlike the exponentially suppressed gap in the localized regime, which leads to the fidelity of the adiabatic pumping depending on the length of the lattice. To achieve successful pumping in a longer lattice, despite the extended bulk modes of the system, a slower variation of φ is needed to avoid the Landau-Zener tunneling from the bulk subchannel to its adjacent sublevel during evolution.

IV. ANOMALOUS EXCITATION TRANSFER AND NONRECIPROCAL TRANSPORT

The adiabatic pumping between the left and right edge modes could be potentially exploited in the transfer between excitations at both boundaries of the lattice, namely, quantum state transfer. To this end, we consider the initial state injected into the leftmost (rightmost) site for channel A (B). Because each edge mode is mainly concentrated on either side of the sample system, both the initial states mostly contain a superposition of a corresponding edge mode, and the excitation transfer purely depends on the pumping process between the left and right edge modes. As shown in Fig. 4(a1), for both channels, the adiabatic evolution is in the same direction and we slowly ramp φ from 0.39π to 1.39π, with $\varphi = 0.39\pi + \Omega t$. The corresponding evolution processes after resorting to channels A and B are reported in Figs. 4(a2) and 4(a3), respectively. It is evident that an excitation is transferred to the other side of the sample system whether it is initially injected from the leftmost or rightmost site, but the transfer outcome is imperfect; in other words, the transferred excitation is not entirely localized on the opposite boundary of the lattice.

Similarly, we quantify the transfer outcome by employing the fidelity, Eq. (4), where the goal state $|\Psi_g\rangle$ is chosen as the
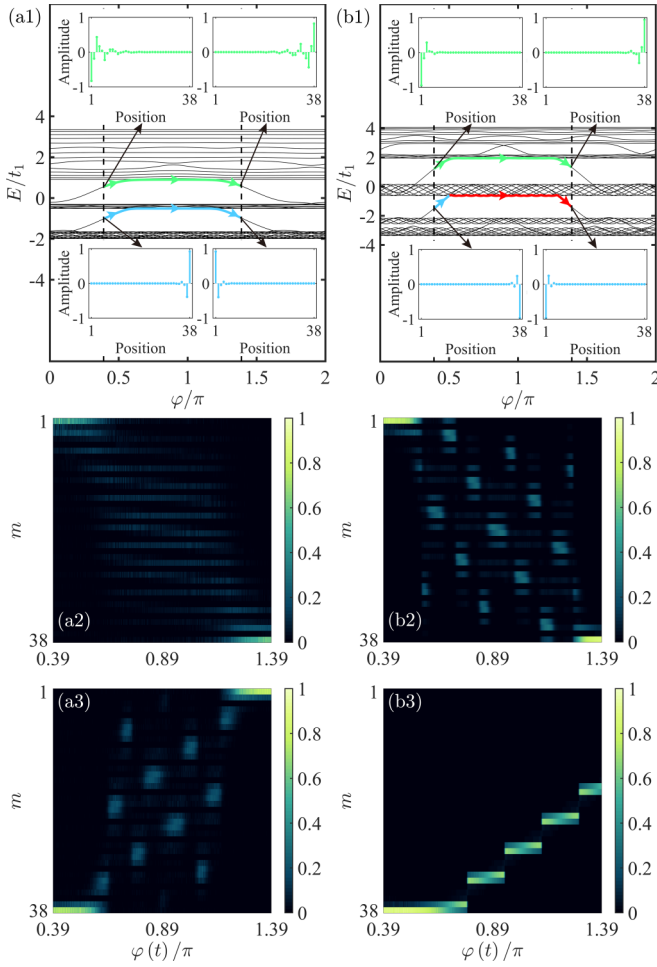
FIG. 4. Energy spectrum of the sample system with the number of sites $N = 38$ as a function of modulation phase φ for (a1) $V = 1.4$ and (b1) $V = 3$. For the two channels, the adiabatic evolution is in the same direction and within the same region $\varphi \in [0.39\pi, 1.39\pi]$, as shown between the black dashed lines. The insets in (a1) and (b1) display the left and right edge modes at $\varphi = 0.39\pi$ and 1.39π. In (a1), both the channels remain intact, which results in a bidirectional transfer between excitations at both boundaries of the lattice, as reported in (a2) and (a3). In (b1), only channel A remains intact, and channel B collapses, which brings about a nonreciprocal transport manifested by the unidirectional excitation transfer, as reported in (b2) and (b3). The color bar indicates the density on each site during evolution and $\Omega = 10^{-5}$ in all the evolution processes.

FIG. 5. Fidelity F of the excitation transfer in the sample system versus modulation strength V and ramping frequency Ω via (a) channel A and (b) channel B. The white dashed line in both plots delineates the threshold V_c of the corresponding bulk subchannel, which is almost equal to that extracted from Fig. 1. (c) In channel A, $|\psi_1|$ of the left edge mode at $\varphi = 0.39\pi$ and $|\psi_N|$ of the right edge mode at $\varphi = 1.39\pi$ as a function of modulation strength V. (d) In channel B, $|\psi_N|$ of the right edge mode at $\varphi = 0.39\pi$ and $|\psi_1|$ of the left edge mode at $\varphi = 1.39\pi$ as a function of modulation strength V.

state injected into the rightmost (leftmost) site for channel A (B). Figures 5(a) and 5(b) exhibit the fidelities F of channels A and B versus V and Ω for the sample system, respectively. We can observe that for both channels, the occurrence of the Anderson localization also has an adverse effect on the excitation transfer caused by the collapse of the adiabatic pumping, which is feasible until the corresponding bulk subchannel undergoes the localization-delocalization transition. In the delocalized regime, we find that with the increase of V and the decrease of Ω, fidelity rises, which, in a sense, implies that the enhanced quasidisorder is conducive to the excitation transfer. This is unique for quasidisorder since increasing stochastic disorder strength will gradually eliminate the relevant gap
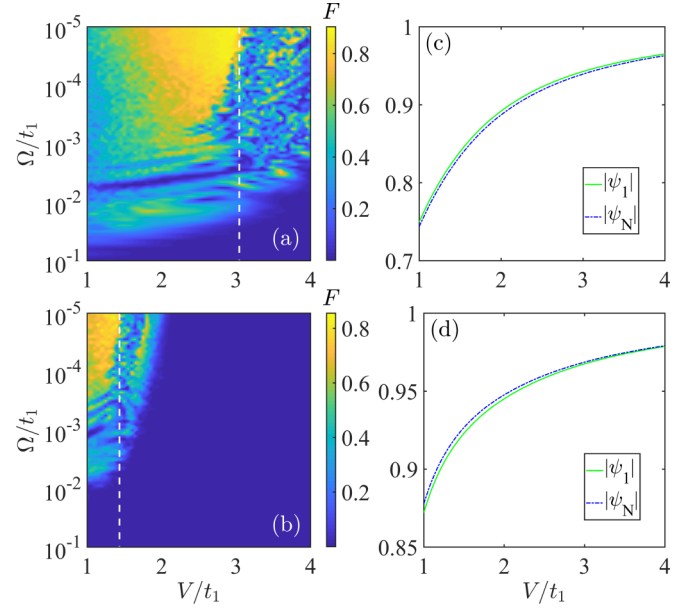
and is generally not beneficial to quantum state transfer. The reason behind this phenomenon is ascribed to the fact that the increasing quasidisorder strength V enhances the localization of each edge mode on the corresponding boundary of the lattice, as displayed in Fig. 5(c) [Fig. 5(d)] for $|\psi_1|$ ($|\psi_N|$) of the left (right) edge mode at $\varphi = 0.39\pi$ and $|\psi_N|$ ($|\psi_1|$) of the right (left) edge mode at $\varphi = 1.39\pi$, so that the weight of the left (right) edge mode in the eigenmode superposition of the initial state for channel A (B) is elevated. As a consequence, as V increases, although the relevant gap also gradually diminishes, when Ω is small enough, the pumping process between the left and right edge modes is more and more dominant in the whole adiabatic evolution, which contributes to receiving a final state that is more localized on the other boundary of the lattice and further to a higher fidelity and thus to the anomalous excitation transfer.

Another interesting phenomenon exists in the scope of $1.434 < V < 3.042$, viz., before the Anderson localization for the bulk subchannel of channel A occurs and after the bulk subchannel of channel B undergoes the localization-delocalization transition. It turns out that if we initially inject an excitation into the leftmost site, it can be adiabatically transferred to the opposite side of the sample system by scanning φ sufficiently slowly except that the transferred excitation is output incompletely from the rightmost site; nevertheless, when an excitation is initially injected into the rightmost site and φ is slowly swept again within the same range, it is possible for the excitation not to be output at all from the leftmost site, which arises from the presence

of the mobility edge triggering the opposite outcome of the adiabatic pumping in this scope for channels A and B and can be treated as a nonreciprocal effect, as shown in Fig. 4(b1). The nonreciprocal effect will become more pronounced with V approaching 3.042, as reported in Figs. 4(b2) and 4(b3) with $V = 3$, and cannot emerge in the AA model. Based on the nonreciprocal transport across the bulk induced by the mobility edge, it is feasible to engineer a quantum diode by viewing both the leftmost and rightmost sites as two ports.

V. CONCLUSIONS

In conclusion, we have investigated the quantum transport in a 1D quasicrystal with a specific short-range hopping, i.e., the adiabatic pumping between left and right edge modes and the transfer between excitations at both boundaries of the lattice. The quasiperiodic lattice is described by an exponentially decaying hopping and sustains energy-dependent mobility edges. The adiabatic pumping can be implemented by resorting to two channels and is always feasible before the occurrence of the Anderson localization of the corresponding bulk subchannel, which results from the exponentially suppressed gap in the localized regime leading to the Landau-Zener tunneling between sublevels. Therefore, for both channels, successful pumping in the AA model can be achieved until the system undergoes the localization-delocalization transition, viz., when $V < 2$. Compared with the AA model, the introduction of mobility edges increases

(decreases) the threshold of the transition for the bulk subchannel of channel A (B), which brings about a different outcome for the adiabatic pumping in the two channels. In other words, successful pumping in channel A persists even after $V > 2$, but in channel B it survives only with a reduced critical condition. If we interpret the incommensurate on-site potential as a highly correlated disorder, overall, it turns out that the presence of mobility edges actually facilitates the robustness of the adiabatic pumping against quasidisorder. Furthermore, depending on the pumping process, we have shown that the transfer between excitations at both boundaries of the lattice is anomalous in the delocalized regime, which is characterized by the enhanced quasidisorder elevating the fidelity of the excitation transfer. Moreover, there exists a parametric regime where a nonreciprocal effect emerges. The nonreciprocal effect results in unidirectional transport for the excitation transfer, which is absent in the AA model. Based on the nonreciprocal transport, a promising application could be the exploitation and preparation of quantum diodes.

Although the present work focused on adiabatic evolution, we also hope that more interest can be stimulated for the exploration of quantum transport in quasicrystals based on active controls, such as shortcuts to adiabaticity.

[1] P. W. Anderson, Phys. Rev. **109**, 1492 (1958).

[2] P. A. Lee and T. V. Ramakrishnan, Rev. Mod. Phys. **57**, 287 (1985).

[3] F. Evers and A. D. Mirlin, Rev. Mod. Phys. **80**, 1355 (2008).

[4] G. Roati, C. D'Errico, L. Fallani, M. Fattori, C. Fort, M. Zaccanti, G. Modugno, M. Modugno, and M. Inguscio, Nature (London) **453**, 895 (2008).

[5] Y. Lahini, R. Pugatch, F. Pozzi, M. Sorel, R. Morandotti, N. Davidson, and Y. Silberberg, Phys. Rev. Lett. **103**, 013901 (2009).

[6] E. Abrahams, P. W. Anderson, D. C. Licciardello, and T. V. Ramakrishnan, Phys. Rev. Lett. **42**, 673 (1979).

[7] D. Levine and P. J. Steinhardt, Phys. Rev. Lett. **53**, 2477 (1984).

[8] V. Elser, Phys. Rev. Lett. **54**, 1730 (1985).

[9] D. Levine and P. J. Steinhardt, Phys. Rev. B **34**, 596 (1986).

[10] J. E. S. Socolar and P. J. Steinhardt, Phys. Rev. B **34**, 617 (1986).

[11] P. G. Harper, Proc. Phys. Soc. London, Sect. A **68**, 874 (1955).

[12] S. Aubry and G. André, Ann. Isr. Phys. Soc. **3**, 133 (1980).

[13] D. R. Hofstadter, Phys. Rev. B **14**, 2239 (1976).

[14] J. Billy, V. Josse, Z. Zuo, A. Bernard, B. Hambrecht, P. Lugan, D. Clément, L. Sanchez-Palencia, P. Bouyer, and A. Aspect, Nature (London) **453**, 891 (2008).

[15] S. S. Kondov, W. R. McGehee, J. J. Zirbel, and B. DeMarco, Science **334**, 66 (2011).

[16] F. Jendrzejewski, A. Bernard, K. Müller, P. Cheinet, V. Josse, M. Piraud, L. Pezzé, L. Sanchez-Palencia, A. Aspect, and P. Bouyer, Nat. Phys. **8**, 398 (2012).

[17] W. R. McGehee, S. S. Kondov, W. Xu, J. J. Zirbel, and B. DeMarco, Phys. Rev. Lett. **111**, 145303 (2013).

[18] J. Biddle, B. Wang, D. J. Priour, and S. Das Sarma, Phys. Rev. A **80**, 021603(R) (2009).

[19] J. Biddle and S. Das Sarma, Phys. Rev. Lett. **104**, 070601 (2010).

[20] J. Biddle, D. J. Priour, B. Wang, and S. Das Sarma, Phys. Rev. B **83**, 075105 (2011).

[21] S. Gopalakrishnan, Phys. Rev. B **96**, 054202 (2017).

[22] T. Liu and H. Guo, Phys. Rev. B **98**, 104201 (2018).

[23] X. Deng, S. Ray, S. Sinha, G. V. Shlyapnikov, and L. Santos, Phys. Rev. Lett. **123**, 025301 (2019).

[24] M. Saha, S. K. Maiti, and A. Purkayastha, Phys. Rev. B **100**, 174201 (2019).

[25] S. Ganeshan, J. H. Pixley, and S. Das Sarma, Phys. Rev. Lett. **114**, 146601 (2015).

[26] T. Liu, H. Y. Yan, and H. Guo, Phys. Rev. B **96**, 174207 (2017).

[27] Y. Wang, X. Xia, L. Zhang, H. Yao, S. Chen, J. You, Q. Zhou, and X. J. Liu, Phys. Rev. Lett. **125**, 196604 (2020).

[28] H. P. Lüschen, S. Scherg, T. Kohlert, M. Schreiber, P. Bordia, X. Li, S. Das Sarma, and I. Bloch, Phys. Rev. Lett. **120**, 160404 (2018).

[29] T. Kohlert, S. Scherg, X. Li, H. P. Lüschen, S. Das Sarma, I. Bloch, and M. Aidelsburger, Phys. Rev. Lett. **122**, 170403 (2019).

[30] F. A. An, K. Padavić, E. J. Meier, S. Hegde, S. Ganeshan, J. H. Pixley, S. Vishveshwara, and B. Gadway, Phys. Rev. Lett. **126**, 040603 (2021).

[31] L. J. Lang, X. Cai, and S. Chen, Phys. Rev. Lett. **108**, 220401 (2012).

[32] Y. E. Kraus and O. Zilberberg, Phys. Rev. Lett. **109**, 116404 (2012).

[33] M. Verbin, O. Zilberberg, Y. E. Kraus, Y. Lahini, and Y. Silberberg, Phys. Rev. Lett. **110**, 076403 (2013).

[34] Y. E. Kraus, Y. Lahini, Z. Ringel, M. Verbin, and O. Zilberberg, Phys. Rev. Lett. **109**, 106402 (2012).

[35] K. A. Madsen, E. J. Bergholtz, and P. W. Brouwer, Phys. Rev. B **88**, 125118 (2013).

[36] J. Alicea, Y. Oreg, G. Refael, F. von Oppen, and M. P. A. Fisher, Nat. Phys. **7**, 412 (2011).

[37] N. Lang and H. P. Büchler, npj Quantum Inf. **3**, 47 (2017).

[38] C. Nayak, S. H. Simon, A. Stern, M. Freedman, and S. Das Sarma, Rev. Mod. Phys. **80**, 1083 (2008).

[39] A. Stern and N. H. Lindner, Science **339**, 1179 (2013).

[40] D. J. Thouless, Phys. Rev. B **27**, 6083 (1983).

[41] S. Nakajima, T. Tomita, S. Taie, T. Ichinose, H. Ozawa, L. Wang, M. Troyer, and Y. Takahashi, Nat. Phys. **12**, 296 (2016).

[42] M. Lohse, C. Schweizer, O. Zilberberg, M. Aidelsburger, and I. Bloch, Nat. Phys. **12**, 350 (2016).

[43] S. Hu, Y. Ke, Y. Deng, and C. Lee, Phys. Rev. B **100**, 064302 (2019).

[44] S. Hu, Y. Ke, and C. Lee, Phys. Rev. A **101**, 052323 (2020).

[45] F. Liu, S. Ghosh, and Y. D. Chong, Phys. Rev. B **91**, 014108 (2015).

[46] X. L. Zhao, Z. C. Shi, C. S. Yu, and X. X. Yi, J. Phys. B **50**, 235503 (2017).

[47] M. Verbin, O. Zilberberg, Y. Lahini, Y. E. Kraus, and Y. Silberberg, Phys. Rev. B **91**, 064201 (2015).

[48] E. Riva, M. I. N. Rosa, and M. Ruzzene, Phys. Rev. B **101**, 094307 (2020).

[49] E. Riva, V. Casieri, F. Resta, and F. Braghin, Phys. Rev. B **102**, 014305 (2020).

[50] W. Cheng, E. Prodan, and C. Prodan, Phys. Rev. Lett. **125**, 224301 (2020).

[51] Y. Xia, E. Riva, M. I. N. Rosa, G. Cazzulani, A. Erturk, F. Braghin, and M. Ruzzene, Phys. Rev. Lett. **126**, 095501 (2021).

[52] N. Y. Yao, C. R. Laumann, A. V. Gorshkov, H. Weimer, L. Jiang, J. I. Cirac, P. Zoller, and M. D. Lukin, Nat. Commun. **4**, 1585 (2013).

[53] C. Dlaska, B. Vermersch, and P. Zoller, Quantum Sci. Technol. **2**, 015001 (2017).

[54] F. Mei, G. Chen, L. Tian, S. L. Zhu, and S. Jia, Phys. Rev. A **98**, 012331 (2018).

[55] S. Longhi, G. L. Giorgi, and R. Zambrini, Adv. Quantum Technol. **2**, 1800090 (2019).

[56] S. Longhi, Phys. Rev. B **99**, 155150 (2019).

[57] F. M. D'Angelis, F. A. Pinheiro, D. Guéry-Odelin, S. Longhi, and F. Impens, Phys. Rev. Research **2**, 033475 (2020).

[58] I. Brouzos, I. Kiorpelidis, F. K. Diakonos, and G. Theocharis, Phys. Rev. B **102**, 174312 (2020).

[59] L. N. Zheng, L. Qi, L. Y. Cheng, H. F. Wang, and S. Zhang, Phys. Rev. A **102**, 012606 (2020).

[60] L. Qi, G. L. Wang, S. Liu, S. Zhang, and H. F. Wang, Phys. Rev. A **102**, 022404 (2020).

[61] J. Cao, W. X. Cui, X. X. Yi, and H. F. Wang, Phys. Rev. A **103**, 023504 (2021).

[62] L. Qi, Y. Xing, X. D. Zhao, S. Liu, S. Zhang, S. Hu, and H. F. Wang, Phys. Rev. B **103**, 085129 (2021).

[63] J. X. Han, J. L. Wu, Y. Wang, Y. Xia, Y. Y. Jiang, and J. Song, Phys. Rev. A **103**, 032402 (2021).

[64] L. Qi, Y. Yan, Y. Xing, X. D. Zhao, S. Liu, W. X. Cui, X. Han, S. Zhang, and H. F. Wang, Phys. Rev. Research **3**, 023037 (2021).

[65] J. Cao, W. X. Cui, X. Yi, and H. F. Wang, Ann. Phys. (Berlin, Ger.) **533**, 2100120 (2021).

[66] P. Boross, J. K. Asbóth, G. Széchenyi, L. Oroszlány, and A. Pályi, Phys. Rev. B **100**, 045414 (2019).